Collective energy-spectrum broadening of a proton beam in a gas-discharge plasma

Rui Cheng,[1,6,7] Zhang-Hu Hu,[2,*] De-Xuan Hui,[2] Yong-Tao Zhao,[1,3] Yan-Hong Chen,[1] Fei Gao,[2] Yu Lei,[1] Yu-Yu Wang,[1] Bing-Li Zhu,[4] Yang Yang,[4] Zhao Wang,[1,5] Ze-Xian Zhou,[1,5] You-Nian Wang,[2] and Jie Yang[1]

[1]*Institute of Modern Physics, Chinese Academy of Sciences, Lanzhou 730000, China*

[2]*School of Physics, Dalian University of Technology, Dalian 116024, China*

[3]*MOE Key Laboratory for Nonequilibrium Synthesis and Modulation of Condensed Matter, School of Physics, Xi'an Jiaotong University, Xi'an 710049, China*

[4]*Xi'an Institute of Optics and Precision Mechanics, Chinese Academy of Sciences, Xi'an 710049, China*

[5]*College of Physics and Electronic Engineering, Northwest Normal University, Lanzhou 730000, China*

[6]*University of Chinese Academy of Sciences, Beijing 100049, China*

[7]*Advanced Energy Science and Technology Guangdong Laboratory, Huizhou 516003, China*

(Received 30 January 2021; accepted 7 June 2021; published 28 June 2021)

An accurate understanding of ion-beam transport in plasmas is crucial for applications in inertial fusion energy and high-energy-density physics. We present an experimental measurement on the energy spectrum of a proton beam at 270 keV propagating through a gas-discharge hydrogen plasma. We observe the energies of the beam protons changing as a function of the plasma density and spectrum broadening due to a collective beam-plasma interaction. Supported by linear theory and three-dimensional particle-in-cell simulations, we attribute this energy modulation to a two-stream instability excitation and further saturation by beam ion trapping in the wave. The widths of the energy spectrum from both experiment and simulation agree with the theory.

DOI: 10.1103/PhysRevE.103.063216

I. INTRODUCTION

Ion-beam pulses are commonly used in a variety of research fields, such as ion-driven inertial fusion [1,2] and high-energy-density physics research [3,4]. An intense ion beam is proposed to be a new solution to produce large volume high-energy density matter with a homogeneous state because of its long penetration range and a relative constant stopping power along the trajectory. With the development of high-intensity lasers, the required ion beams can be produced from laser-plasma interactions, in which the beam usually has a large divergence and needs to be focused before it is delivered to the target [5]. The ion beam from conventional accelerators also needs to be focused transversely for applications in high-energy-density physics. Simulations [6–9] and experiments [10–15] have proven that a background plasma can be provided as an effective medium for the transport and focusing of intense charged particle beams, due to the effective neutralization of beam space charge by plasma electrons.

However, it should be noted that the ion-beam propagation in a background plasma can be subject to collective instabilities, which have important impacts on the beam transport and final beam energy spectrum. For nonrelativistic beam ions, a longitudinal modulation effect driven by the two-stream instability between beam ions and plasma electrons highlights the main feature [16–18]. The result of the instability is to produce short-wavelength electrostatic wave perturbations with a frequency close to the plasma frequency $\omega \approx \omega_{pe}$. The unstable wave has a phase velocity which is close to the beam velocity and saturates either by the longitudinal trapping of plasma electrons in the wave, which happens when the electron's amplitude of the velocity oscillation in the wave becomes of order of the phase velocity of the wave, or by the trapping of beam ions, which happens when the beam ion's amplitude of the velocity oscillation in the wave becomes of order of the difference between the beam velocity and the phase velocity of the wave. If the saturation is caused by beam ion trapping, the beam density becomes highly modulated in the longitudinal direction and the beam splits longitudinally into short bunches with length $\approx v_b/\omega_{pe} \ll l_b$, where v_b and l_b are the initial beam velocity and length.

It is shown that for long, nonrelativistic beams, the charge neutralization is very good even for a tenuous background plasma with a density much smaller than the beam density [7]. The electrostatic two-stream instability for a cold, longitudinally compressing charged particle beam propagating through a background plasma has been investigated both analytically and numerically [19]. In addition, simulations [16,18,20] show that the two-stream instability can play a significant role in the ion-beam dynamics and leads to a transverse defocusing of the beam ions. The long-time evolution of the two-stream instability and generation of a forerunner electron beam during beam-plasma interactions are also investigated in detail using large-scale one-dimensional electrostatic kinetic simulations [21]. Although a growing body of literature has been dedicated to studying collective beam-plasma interactions, little experimental work has been performed at present to investigate the ion-beam excited two-stream instability, especially the instability saturation due to beam ion trapping. In

*zhanghu@dlut.edu.cn

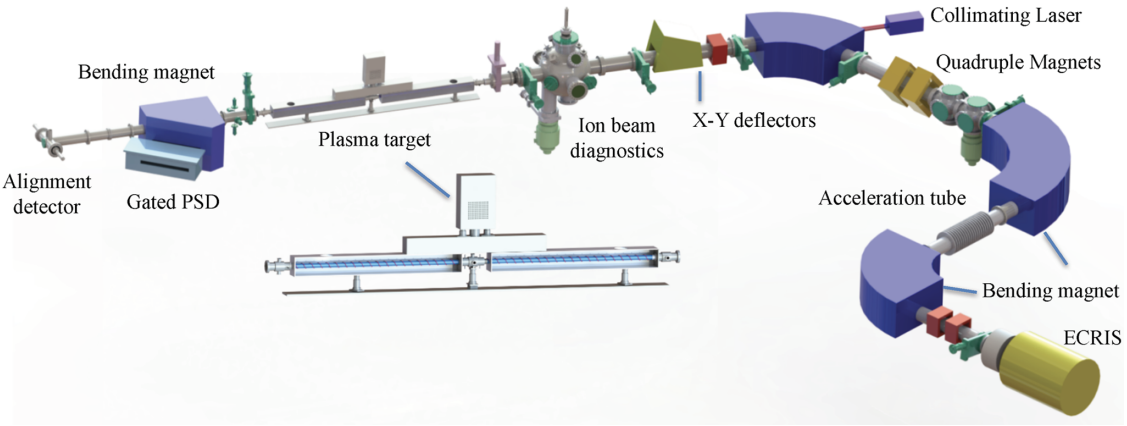

FIG. 1. Experimental layout. The proton beams from the ECR ion source were accelerated and delivered to a radio-frequency inductively coupled plasma target. After the plasma device, a bending magnet with 45° deflection over a 0.5 m radius and a position-sensitive detector were employed to measure the beam energy.

this paper, with a specially designed 2.2-m-long low-density gas-discharge plasma device, we perform an experimental study of proton-beam excited two-stream instability. With properly selected beam and plasma parameters, a collective broadening of the beam energy spectrum at the plasma exit is clearly observed due to the beam ion trapping in the wave, which is confirmed by linear theory and three-dimensional particle-in-cell (3D PIC) simulations. The paper is organized as follows: In Sec. II the experimental setup is described, and the results are discussed in Sec. III. Finally, conclusions are given in Sec. IV.

II. EXPERIMENTAL SETUP

The ion-plasma interaction experimental setup was constructed at the 320-kV high-voltage platform at the Institute of Modern Physics, Chinese Academy of Sciences (IMPCAS) in Lanzhou [22] as indicated in Fig. 1. Proton- and heavy-ion beams with currents from 100 e nA to 100 $e\,\mu$A can be produced by the electron cyclotron resonance (ECR) ion source. After two 90° bending magnets, the X-Y deflectors and several quadrupole magnets were used to deliver the beams to the plasma target. The energy spread of the beam is less than 0.3%. A 2.2-m-long radio-frequency (rf) inductively coupled plasma target (the small inset figure in Fig. 1) was installed and the homogenous plasma was generated by the 13.56 MHz rf power varying from 100 to 1000 W. Pure (99.999%) hydrogen gas was filled into the quartz tubes, each 1.0 m long, through a metallic needle valve in the middle of target, where a capacitance diaphragm vacuum gauge of CDG 500 was used to monitor the interior gas density. The working pressure can be changed from 5 to 50 Pa. The plasma electron density can be changed from 10^{15} to 10^{17} m^{-3} and temperature from 4 to 9 eV. Figure 2 shows the density and temperature of the hydrogen plasma as a function of the rf power in different pressure conditions. In the experiment, the plasma parameters were diagnosed offline by the dual-Langmuir probe. Considering the long distance of the rf plasma itself, a specially designed alignment and positioning system was developed. A collimating laser from a second bending magnet to the straight end of the beamline was used to align the plasma device.

In order to retain the high vacuum condition in both external ends of the plasma, a two-stage differential pumping system consisting of two turbopumps (evacuation rate 300 l/s) and a roof pump (evacuation rate 8 l/s) were employed, where the beamline and the plasma target were separated by four apertures with a diameter of 2 mm and a length of 20 mm. Each stage can reduce the pressure by a factor of 100, and the base pressure along the beamline stays at 10^{-5} Pa when the gas pressure in the rf plasma target is about 5 Pa. The ion beams windowlessly penetrate through the plasma, which ensures a low beam energy spread before the ion beam-plasma interaction. After the plasma device, a bending magnet with 45° deflection over a 0.5 m radius and a position-sensitive detector (PSD) were employed to measure the energy of protons. The maximum of magnetic field intensity is about 0.3 T and the current instability is less than 0.03%. The PSD consists of a gated microchannel plate (MCP) detector, a phosphor screen, and a rear CCD camera, which has a spatial resolution of about 70 μm. A four-slit diaphragm in front of the bending magnet gives the up limit of beam size less than 0.2×0.2 mm^2 and the high-energy resolution can be achieved.

III. RESULTS

Figure 3 shows the energy spectrum of beam protons with an initial energy 270 keV for the following cases: (a) plasma off (i.e., neutral hydrogen gas of pressure 5 Pa), (b) plasma on with rf power 900 W and free-electron density 5.2×10^{16} m^{-3}, and (c) plasma on with rf power 1000 W and free-electron density 5.8×10^{16} m^{-3}. It is obviously the beam energy moves to the "loss" side when the target is filled with hydrogen gas of pressure 5 Pa and the energy loss is about 1.0 keV. Once the hydrogen gas is ignited to the plasma state, the energy spread of the proton beam increases significantly and a two-peak structure in the energy spectrum can be observed, as indicated in Fig. 3(c). The width of the two-peak structure is shown to be 1.0 keV, with one peak located at 269 keV, which is the position of beam energy in the cold gas [Fig. 3(a)], and the other one located at 270 keV. This energy-spectrum broadening cannot be explained by the

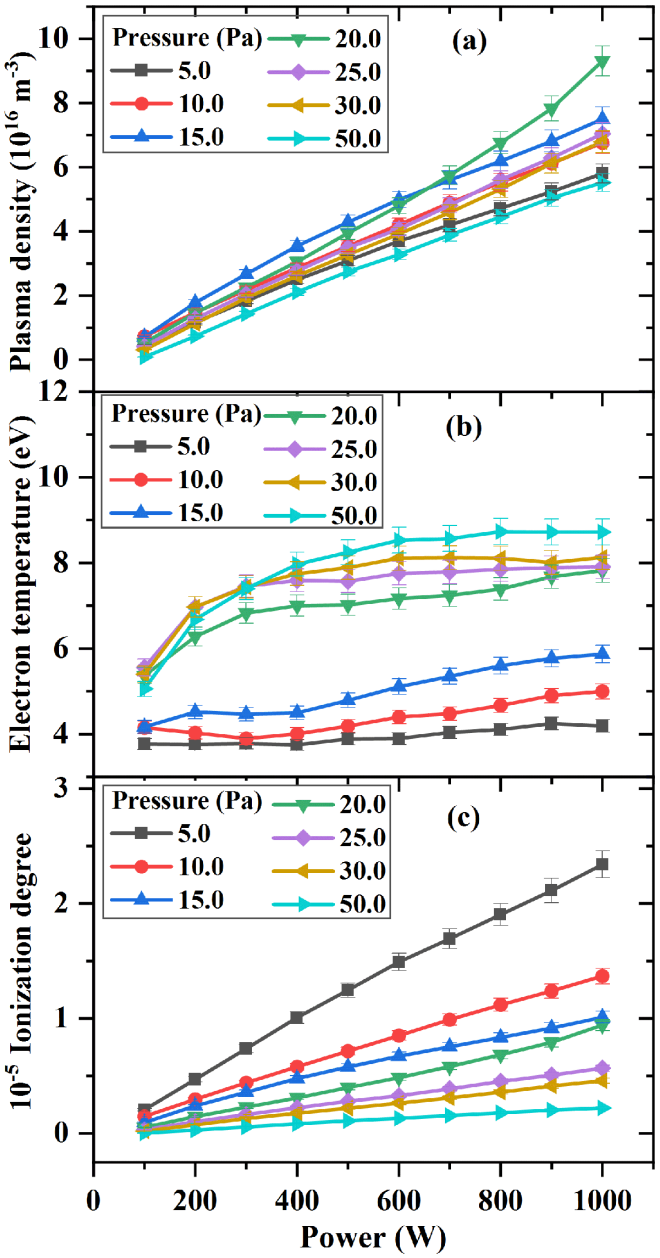

FIG. 2. (a) Hydrogen plasma density and (b) electron temperature as a function of the rf power in different pressure conditions. The plasma parameters were diagnosed offline by the dual-Langmuir probe. (c) The ionization degree of the plasma target is also shown in the figure.

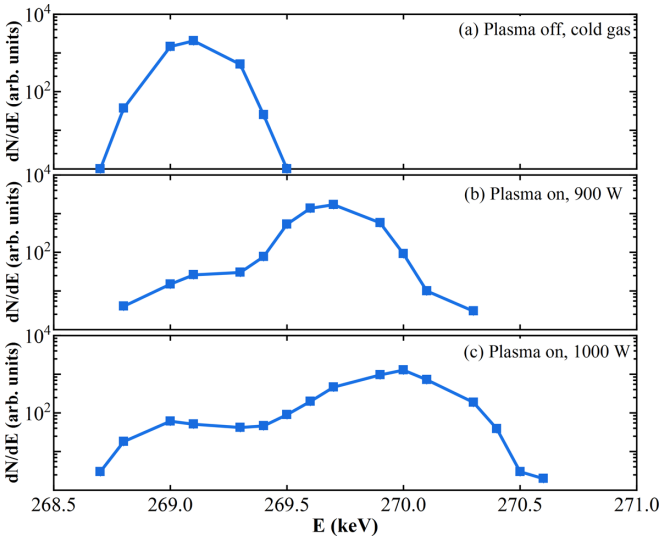

FIG. 3. Experimental result. Energy spectrum of beam protons with an initial energy 270 keV for the following cases: (a) plasma off (i.e., neutral hydrogen gas of pressure 5 Pa), (b) plasma on with rf power 900 W and free-electron density 5.2×10^{16} m^{-3}, and (c) plasma on with rf power 1000 W and free-electron density 5.8×10^{16} m^{-3}. The error bars in the figure are undistinguishable and the measurement error range is below 10%.

collision model, i.e., the collision between beam protons and plasma electrons. With a plasma density of 5.8×10^{16} m^{-3}, the collisions between beam protons of energy 270 keV and plasma electrons can be neglected and the collective beam-plasma interactions need to be considered.

For the beam and plasma parameters in the experiment, the wakefield and two-stream instability (between the beam protons and plasma electrons) can be excited and becomes saturated, as indicated below. The dispersion relation of the two-stream instability of a monoenergetic beam interacting with a plasma, neglecting the beam's own magnetic field, is given by

$$1 - \frac{\omega_{pe}^2}{\omega(\omega + i\nu)} - \frac{1}{\Gamma^2}\frac{\omega_b^2}{\Omega^2}(\Gamma^2 \sin^2\phi + \cos^2\phi) = 0, \qquad (1)$$

where ω_b is the ion-beam frequency, $\Omega = \omega - \vec{k}\cdot\vec{v}_b$ is the Doppler-shifted wave frequency, Γ the Lorentz factor of beam protons, and ϕ is the angle between the wave vector $\vec{k}$ and the beam velocity $\vec{v}_b$, i.e., $\vec{k}\cdot\vec{v}_b = kv_b\cos\phi = k_\parallel v_b$. With a plasma density of 5.8×10^{16} m^{-3}, the plasma electron collision frequency ν and oscillation frequency ω_{pe} are estimated to be 4×10^8 s^{-1} and 1.3×10^{10} s^{-1}, respectively. Therefore, the plasma can be considered to be collisionless with $\nu \ll \omega_{pe}$. The peak growth occurs at $k_\parallel v_b = \omega_{pe}$ and is given by

$$\gamma = \mathrm{Im}\,\omega = \frac{\sqrt{3}}{2}\omega_b\left(\frac{\omega_{pe}}{2\omega_b}\frac{(\Gamma^2\sin^2\phi + \cos^2\phi)}{\Gamma^2}\right)^{1/3}. \qquad (2)$$

For the beam energy in this work, the Lorentz factor $\Gamma \approx 1$ and the growth rate of the two-stream instability is $\gamma/\omega_{pe} = 0.69(\frac{n_b}{n_e}\frac{m_e}{m_b})^{1/3}$, where n_b and n_e are the density of the proton beam and plasma electrons, respectively. The beam density n_b in our experiments is estimated to be 2.8×10^{11} m^{-3} with a current of 1 μA and radius 1 mm. With a plasma electron density of 5.8×10^{16} m^{-3}, the growth rate is shown to be $\gamma/\omega_{pe} \approx 9.5 \times 10^{-4}$ and the characteristic plasma length for the two-stream instability to grow is $L_c = v_b\gamma^{-1} \approx 0.56$ m. Therefore, it is expected that an instability develops and saturates after a travel distance of 2.2 m in the background plasma.

For the beam and plasma parameters in the experiments, we have $[(m_b/m_e)(n_b/n_e)^2]^{1/3} < 1$ and the saturation is caused by beam ion trapping, in which the beam ion's amplitude of velocity oscillation in the wave becomes of order of the difference between the beam velocity and the phase

velocity of the wave $v_m^b \sim v_b - \omega/k_\parallel \sim \gamma/k_\parallel \approx (\gamma/\omega_{pe})v_b$. Here, we used the fact that $\omega - k_\parallel v_b \sim \gamma$. From this, the width of the two-peak structure in the beam energy spectrum can be estimated as $\Delta E = m_b(v_b + v_m^b)^2/2 - m_b(v_b - v_m^b)^2/2 = 2m_b v_b v_m^b \approx 1.026$ keV, which shows good agreement with the experiment result. It should be noted that the beam proton stopping and energy transfer to plasma electrons and ions are not significant in this case due to the trapping of beam protons, not plasma electrons. In addition, with a plasma density of about 5.8×10^{16} m^{-3} the plasma skin depth is about 2.2 cm, which is much larger than the radius of the proton beam (1 mm). Therefore, the excitation of the current filamentation instability [23,24] between beam protons and plasma electrons can be neglected.

Three-dimensional electrostatic PIC simulations with the code BPVLAB [25] are also performed here to show this modulation effect. The dimensional effect (2D vs 3D) in PIC simulations is a well-known issue that affects the quantitative results significantly. Especially for beam-plasma interactions, the magnitudes of the longitudinal and transverse wakefields excited by the beam in plasmas will change a lot from 2D to 3D simulations, and therefore the magnitude of beam modulation. With this consideration, full 3D PIC simulations are performed. The beam and plasma parameters adopted in the simulation are the same as in the experiment, except for the beam density n_b, which is set to be 10^{15} m^{-3} to reduce the numerical noise and simulation length. Although the beam density is higher than that in the experiment, the parameter $[(m_b/m_e)(n_b/n_e)^2]^{1/3} \approx 0.8 < 1$ and the saturation is still caused by beam ion trapping. The 3D simulation has a total of $64 \times 64 \times 4096$ cells, with a grid cell of $h_x = h_y = h_z = 6.17 \times 10^{-5}$ m and a time step of $\Delta t = 4.29 \times 10^{-12}$ s. In the simulation the beam propagates along the z-axis direction. For the beam and plasma parameters in the simulation, the growth rate is $\gamma/\omega_{pe} \approx 1.46 \times 10^{-2}$ and the characteristic length for the instability to grow is $L_c = v_b\gamma^{-1} \approx 3.6$ cm. With a plasma length $L = 4096 \times h_z = 25.3$ cm, the instability develops and becomes saturated as indicated in Fig. 4, in which the beam density and longitudinal phase space distribution $(z - v_z)$ after a travel distance of 25 cm are displayed. From Fig. 4(a), the continuous proton beam is highly modulated and splits longitudinally into short bunches. The density of the short bunches reaches 3.5×10^{16} m^{-3} and is 35 times higher than the initial beam density. The instability saturation due to beam ion trapping in the wave can also be observed in Fig. 4(b). As indicated previously, the beam proton's amplitude of velocity oscillation in the wave is $v_m^b \approx (\gamma/\omega_{pe})v_b = 1.05 \times 10^5$ m/s. From Fig. 4(b), the difference between the maximum (about 7.25×10^6 m/s) and minimum (about 7.05×10^6 m/s) beam velocity is 2×10^5 m/s (i.e., $\approx 2v_m^b$), showing agreement with the theory. It should be noted here that we also perform simulations with a higher beam density (i.e., 10^{16} m^{-3}), in which the parameter $[(m_b/m_e)(n_b/n_e)^2]^{1/3} > 1$ and the saturation is due to plasma electron trapping. In this case, the beam density modulation is weaker and the magnitude of the beam velocity oscillation is smaller.

The corresponding energy spectrum of beam protons at the plasma exit is shown in Fig. 5, in which the initial spectrum is also displayed for comparison. The broadening of the spectrum due to a collective beam-plasma interaction and the resulting two-peak structure can be clearly observed in the figure. The widths of the two peaks from simulation and theory estimation are 16 keV and $\Delta E = 2m_b v_b v_m^b \approx 15.8$ keV, respectively, showing agreement with each other.

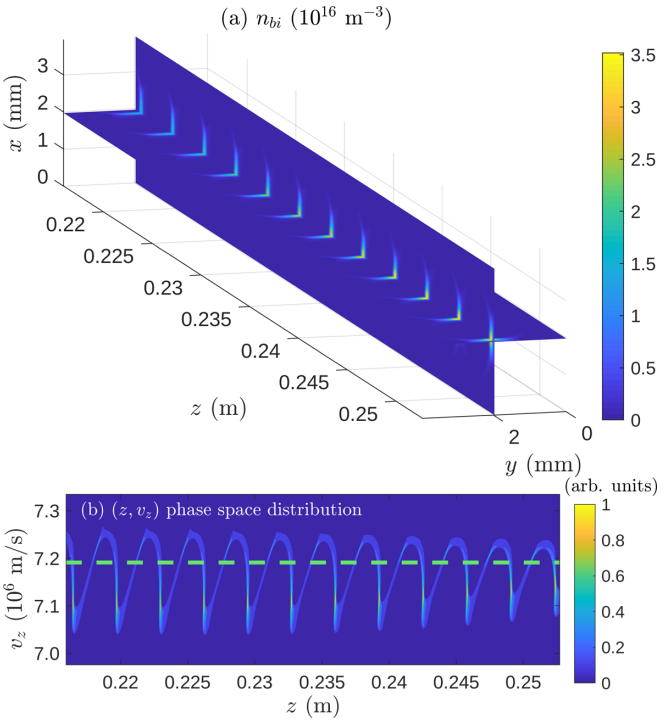

FIG. 4. Simulation result. (a) Beam density and (b) longitudinal phase space distributions $(z - v_z)$ after a travel distance of 25 cm in the plasma. In the figure the proton beam propagates along the z-axis direction. The dotted line in (b) indicates the initial beam velocity.

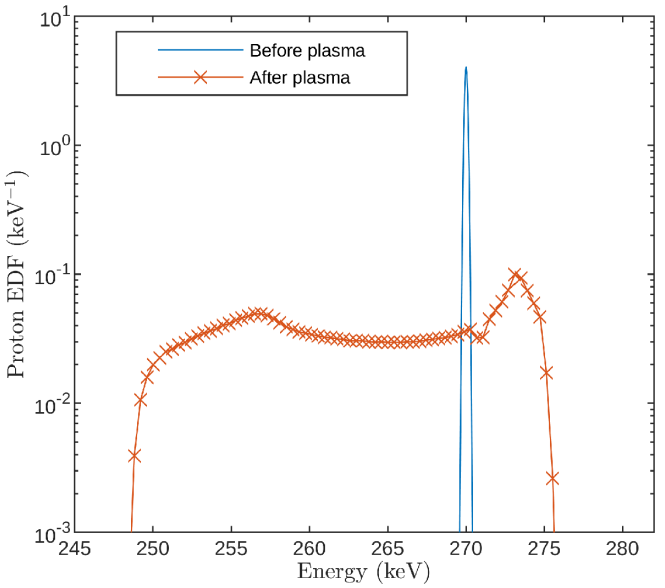

FIG. 5. Energy spectrum of beam protons at the plasma exit from a 3D PIC simulation. The initial beam energy spectrum is also shown in the figure for comparison.

IV. CONCLUSION

In summary, with properly selected beam parameters and a long-living well-characterized plasma device, we show experimentally, supported by linear theory and three-dimensional particle-in-cell simulations, the collective energy-spectrum broadening due to the two-stream instability excitation and saturation by beam ion trapping in the wave. This collective spectrum broadening also confirms the wakefield excitation by the proton beam in the plasma. In the related experiments, the detection of the energy spectrum is an important diagnostic tool. Our results provide an important reference for the experimental investigation of collective beam-plasma interactions. Especially, nowadays the current and energy of ion beams increase significantly with the development of high-intensity lasers (e.g., proton beams from laser-plasma interactions), and beam-plasma instability (e.g., the two-stream instability for ion beams) diagnosis is an important issue for actual beam applications. Although with a higher beam and plasma density in this case, the parameter $[(m_b/m_e)(n_b/n_e)^2]^{1/3}$ may be similar to the low plasma density case in this work and therefore collective energy-spectrum broadening due to beam ion trapping can still be observed. However, the width of the beam energy spectrum ΔE may be different due to collisions in high-density plasmas, which should be investigated in detail.

ACKNOWLEDGMENTS

This work was supported by the National Key R&D Program of China (Grant No. 2017YFA0402300), and National Natural Science Foundation of China (No. 11775042, No. 11775278, No. 11875096, No. 12075046, No. U1532263, and No. U1832175).

[1] P. K. Roy, S. S. Yu, E. Henestroza, A. Anders, F. M. Bieniosek, J. Coleman, S. Eylon, W. G. Greenway, M. Leitner, B. G. Logan, W. L. Waldron, D. R. Welch, C. Thoma, A. B. Sefkow, E. P. Gilson, P. C. Efthimion, and R. C. Davidson, Phys. Rev. Lett. **95**, 234801 (2005).

[2] S. Yu, R. Abbott, R. Bangerter, J. Barnard, R. Briggs, D. Callahan, C. Celata, R. Davidson, C. Debonnel, S. Eylon, A. Faltens, A. Friedman, D. Grote, P. Heitzenroeder, E. Henestroza, I. Kaganovich, J. Kwan, J. Latkowski, E. Lee, B. Logan *et al.*, Nucl. Instrum. Methods Phys. Res., Sect. A **544**, 294 (2005).

[3] N. A. Tahir, D. H. H. Hoffmann, A. Kozyreva, J. A. Maruhn, U. Neuner, A. Tauschwitz, P. Spiller, A. Shutov, and R. Bock, Phys. Rev. E **61**, 1975 (2000).

[4] R. P. Drake, *High-Energy-Density Physics* (Springer, Berlin, 2006).

[5] T. Bartal, M. E. Foord, C. Bellei, M. H. Key, K. A. Flippo, S. A. Gaillard, D. T. Offermann, P. K. Patel, L. C. Jarrott, D. P. Higginson, M. Roth, A. Otten, D. Kraus, R. B. Stephens, H. S. McLean, E. M. Giraldez, M. S. Wei, D. C. Gautier, and F. N. Beg, Nat. Phys. **8**, 139 (2012).

[6] P. Chen, J. J. Su, T. Katsouleas, S. Wilks, and J. M. Dawson, IEEE Trans. Plasma Sci. **15**, 218 (1987).

[7] I. D. Kaganovich, G. Shvets, E. Startsev, and R. C. Davidson, Phys. Plasmas **8**, 4180 (2001).

[8] D. R. Welch, D. V. Rose, B. V. Oliver, and R. E. Clark, Nucl. Instrum. Methods Phys. Res., Sect. A **464**, 134 (2001).

[9] I. D. Kaganovich, E. Startsev, and R. C. Davidson, Phys. Plasmas **11**, 3546 (2004).

[10] G. Hairapetian, P. Davis, C. E. Clayton, C. Joshi, S. C. Hartman, C. Pellegrini, and T. Katsouleas, Phys. Rev. Lett. **72**, 2403 (1994).

[11] R. Govil, W. P. Leemans, E. Yu. Backhaus, and J. S. Wurtele, Phys. Rev. Lett. **83**, 3202 (1999).

[12] J. S. T. Ng, P. Chen, H. Baldis, P. Bolton, D. Cline, W. Craddock, C. Crawford, F. J. Decker, C. Field, Y. Fukui, V. Kumar, R. Iverson, F. King, R. E. Kirby, K. Nakajima, R. Noble, A. Ogata, P. Raimondi, D. Walz, and A. W. Weidemann, Phys. Rev. Lett. **87**, 244801 (2001).

[13] E. Henestroza, S. Eylon, P. K. Roy, S. S. Yu, A. Anders, F. M. Bieniosek, W. G. Greenway, B. G. Logan, R. A. MacGill, D. B. Shuman, D. L. Vanecek, W. L. Waldron, W. M. Sharp, T. L. Houck, R. C. Davidson, P. C. Efthimion, E. P. Gilson, A. B. Sefkow, D. R. Welch, D. V. Rose *et al.*, Phys. Rev. ST Accel. Beams **7**, 083501 (2004).

[14] P. K. Roy, S. S. Yu, S. Eylon, E. Henestroza, A. Anders, F. M. Bieniosek, W. G. Greenway, B. G. Logan, W. L. Waldron, D. L. Vanecek, D. R. Welch, D. V. Rose, R. C. Davidson, P. C. Efthimion, E. P. Gilson, A. B. Sefkow, and W. M. Sharp, Phys. Plasmas **11**, 2890 (2004).

[15] A. Marocchino, M. P. Anania, M. Bellaveglia, A. Biagioni, S. Bini, F. Bisesto, E. Brentegani, E. Chiadroni, A. Cianchi, M. Croia, D. Di Giovenale, M. Ferrario, F. Filippi, A. Giribono, V. Lollo, M. Marongiu, A. Mostacci, G. Di Pirro, R. Pompili, S. Romeo, A. R. Rossi, J. Scifo *et al.*, Appl. Phys. Lett. **111**, 184101 (2017).

[16] R. N. Sudan, Phys. Rev. Lett. **37**, 1613 (1976).

[17] T. C. Genoni, D. V. Rose, D. R. Welch, and E. P. Lee, Phys. Plasmas **11**, L73 (2004).

[18] E. A. Startsev, I. D. Kaganovich, and R. C. Davidson, Nucl. Instrum. Methods Phys. Res., Sect. A **733**, 80 (2014).

[19] E. A. Startsev and R. C. Davidson, Phys. Plasmas **13**, 062108 (2006).

[20] E. Tokluoglu and I. D. Kaganovich, Phys. Plasmas **22**, 040701 (2015).

[21] K. Hara, I. D. Kaganovich, and E. A. Startsev, Phys. Plasmas **25**, 011609 (2018).

[22] R. Cheng, X. Zhou, Y. Wang, Y. Lei, Y. Chen, X. Ma, G. Xiao, Y. Zhao, J. Ren, D. Huo, H. Peng, S. Savin, R. Gavrilin, I. Roudskoy, and A. Golubev, Laser Part. Beams **36**, 98 (2018).

[23] A. Bret, M.-C. Firpo, and C. Deutsch, Phys. Rev. E **70**, 046401 (2004).

[24] A. Bret, M.-C. Firpo, and C. Deutsch, Phys. Rev. Lett. **94**, 115002 (2005).

[25] D. X. Hui, Z. H. Hu, Y. T. Zhao, R. Cheng, X. X. Mei, and Y. N. Wang, Phys. Plasmas **26**, 093104 (2019).